Article

Chemical Reactivity of *D* C (Metallo)Fullerene: Regioselectivity Changes Induced by Sc N Encapsulation

Sílvia Osuna, Marcel Swart, Josep M. Campanera, Josep M. Poblet, and Miquel Solà

More About This Article

Additional resources and features associated with this article are available within the HTML version:

- Supporting Information
- Links to the 2 articles that cite this article, as of the time of this article download
- Access to high resolution figures
- Links to articles and content related to this article
- Copyright permission to reproduce figures and/or text from this article

View the Full Text HTML

Chemical Reactivity of D_{3h} C$_{78}$ (Metallo)Fullerene: Regioselectivity Changes Induced by Sc$_3$N Encapsulation

Sílvia Osuna,[†] Marcel Swart,*,[†,‡] Josep M. Campanera,[§] Josep M. Poblet,[∥] and Miquel Solà*,[†]

Institut de Química Computacional and Departament de Química, Universitat de Girona, Campus Montilivi, 17071 Girona, Catalonia, Spain, Institució Catalana de Recerca i Estudis Avançats (ICREA), Pg. Lluís Companys 23, 08010 Barcelona, Catalonia, Spain, Departament de Fisicoquímica, Facultat de Farmàcia, Universitat de Barcelona, Av. Joan XXIII, s/n, Diagonal Sud, 08028 Barcelona, Catalonia, Spain, and Departament de Química Física i Inorgànica, Universitat Rovira i Virgili, C/ Marcel·lí Domingo, s/n, Campus Sescelades, 43007 Tarragona, Catalonia, Spain

Received December 17, 2007; E-mail: marcel.swart@udg.edu; miquel.sola@udg.edu

Abstract: We report here for the first time a full comparison of the exohedral reactivity of a given fullerene and its parent trinitride template endohedral metallofullerene. In particular, we study the thermodynamics and kinetics for the Diels−Alder [4 + 2] cycloaddition between 1,3-butadiene and free D_{3h}-C$_{78}$ fullerene and between butadiene and the corresponding endohedral D_{3h}-Sc$_3$N@C$_{78}$ derivative. The reaction is studied for all nonequivalent bonds, in both the free and the endohedral fullerenes, at the BP86/TZP//BP86/DZP level. The change in exohedral reactivity and regioselectivity when a metal cluster is encapsulated inside the cage is profound. Consequently, the Diels−Alder reaction over the free fullerene and the endohedral derivative leads to totally different cycloadducts. This is caused by the metal nitride situated inside the fullerene cage that reduces the reactivity of the free fullerene and favors the reaction over different bonds.

Introduction

Soon after the discovery of the C$_{60}$ fullerene structure by Kroto and co-workers[1] in 1985, the possibility of encapsulating metals inside hollow cages was considered. Although Heath et al.[2] presented evidence for the formation of a stable La@C$_{60}$, these so-called endohedral fullerenes[3] could not be produced in high yield until 1999, when Dorn et al.[4] synthesized a new family of endohedral metallofullerenes by using the so-called trimetallic nitride template (TNT) process. This new type of fullerenes contains metal nitrides inside the fullerene, that is, M$_3$N@C$_x$, which results in a formal electronic transfer of six electrons from the M$_3$N unit to the fullerene structure (M$_3$N^{6+}: C$_x^{6-}$). This electron transfer modifies the physical properties and has an enormous influence on the reactivity of these compounds.[5,6]

The first metallofullerene synthesized by Dorn,[4] Sc$_3$N@C$_{80}$, was extremely stable and could be obtained in high yields; as

a matter of fact, the Sc$_3$N@C$_{80}$ compound is the third most abundant fullerene after C$_{60}$ and C$_{70}$. Later, also smaller metallofullerene cages, that is, Sc$_3$N@C$_{78}$ and Sc$_3$N@C$_{68}$, were obtained,[4,7] but in much smaller, yet still reasonable, yields. The Sc$_3$N@C$_{68}$ compound is extraordinary in this respect, because it is one of the few examples of metallofullerenes and the first TNT fullerene that violates the isolated pentagon rule, which states that the most-stable fullerenes should be those where the 12 pentagonal rings are isolated.

The macroscopic quantities in which these TNT compounds were obtained allowed the organic functionalization of these new molecules. This functionalization is important for obtaining nanomaterials with unique properties that might be used in a variety of fields, ranging from molecular electronics to biomedical applications.[6] In 2002, Iezzi et al. reported the crystallographic characterization of the first Diels−Alder derivative of the icosahedral (I_h) isomer of Sc$_3$N@C$_{80}$.[8] This I_h fullerene isomer does not possess the reactive [6,6] pyracylene-type bond (type A in Figure 1, the addition sites of C$_{60}$), and therefore, the reaction took place over a [5,6] corannulene-type bond (type D, Figure 1).

[†] Universitat de Girona.
[‡] ICREA.
[§] Universitat de Barcelona.
[∥] Universitat Rovira i Virgili.

(1) Kroto, H. W.; Heath, J. R.; Obrien, S. C.; Curl, R. F.; Smalley, R. E. *Nature* **1985**, *318*, 162–163.
(2) Heath, J. R.; Obrien, S. C.; Zhang, Q.; Liu, Y.; Curl, R. F.; Kroto, H. W.; Tittel, F. K.; Smalley, R. E. *J. Am. Chem. Soc.* **1985**, *107*, 7779–7780.
(3) Kobayashi, K.; Sano, Y.; Nagase, S. *J. Comput. Chem.* **2001**, *22*, 1353–1358.
(4) Stevenson, S.; Fowler, P. W.; Heine, T.; Duchamp, J. C.; Rice, G.; Glass, T.; Harich, K.; Hajdu, E.; Bible, R.; Dorn, H. C. *Nature* **2000**, *408*, 427–428.
(5) Guha, S.; Nakamoto, K. *Coord. Chem. Rev.* **2005**, *249*, 1111–1132.
(6) Martín, N. *Chem. Commun.* **2006**, 2093–2104.

(7) Olmstead, M. H.; de Bettencourt-Dias, A.; Duchamp, J. C.; Stevenson, S.; Marciu, D.; Dorn, H. C.; Balch, A. L. *Angew. Chem., Int. Ed.* **2001**, *40*, 1223–1225.
(8) (a) Iezzi, E. B.; Duchamp, J. C.; Fletcher, K. R.; Glass, T. E.; Dorn, H. C. *Nano Lett.* **2002**, *2*, 1187–1190. (b) Lee, H. M.; Olmstead, M. M.; Iezzi, E.; Duchamp, J. C.; Dorn, H. C.; Balch, A. L. *J. Am. Chem. Soc.* **2002**, *124*, 3494–3495. (c) Iezzi, E. B.; Duchamp, J. C.; Harich, K.; Glass, T. E.; Lee, H. M.; Olmstead, M. M.; Bach, A. L.; Dorn, H. C. *J. Am. Chem. Soc.* **2002**, *124*, 524–525.
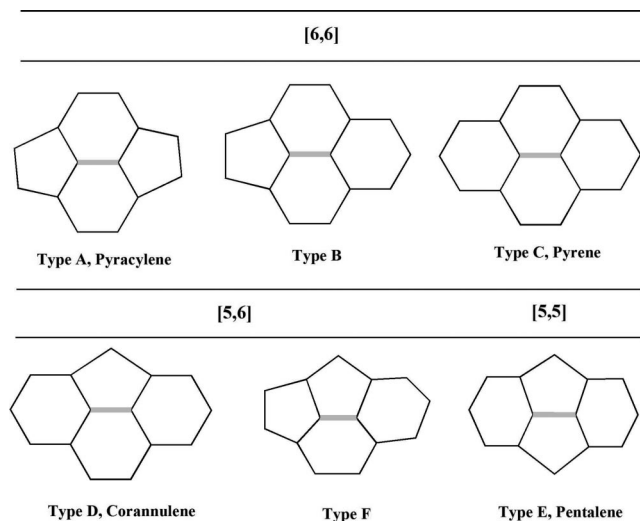
Figure 1. Representation of all possible [6,6], [5,6], and [5,5] bond types that may be present in a fullerene structure.

The first fulleropyrrolidine derivative of I_h-Sc$_3$N@C$_{80}$ was reported in 2005,[9] where a similar reaction pattern (i.e., over [5,6] corannulene-type bonds) was found. For I_h-Y$_3$N@C$_{80}$, the same reaction took place exclusively at a [6,6] bond of type B (Figure 1),[9,10] thus proving that the exohedral chemical reactivity is profoundly affected by the nature of the endohedral metal cluster. Interestingly, ScY$_2$N@C$_{80}$ gives a mixture of [5,6] and [6,6] regioisomers.[11] Dorn and co-workers[12] obtained also a mixture of the [5,6] and [6,6] regioisomers in the synthesis of the *N*-tritylpyrrolidinofullerene when starting from Sc$_3$N@C$_{80}$. The structure of the monoadduct under thermodynamic control was shown, by both NMR spectroscopy and X-ray crystal-lography, to result from addition across the [5,6] ring junction. In contrast, under kinetic control, NMR and X-ray spectroscopy showed conclusively that the product was the [6,6] ring junction adduct. In refluxing chlorobenzene, the [6,6] adduct was converted to the thermodynamically more stable [5,6] isomer. Similar thermal isomerization of the Y$_3$N@(*N*-ethylpyrrolidino-C$_{80}$) leads also to the [5,6] from the [6,6] regioisomer.[13] It was shown by theoretical calculations performed at the BP86/TZP level that this thermal isomerization process takes place through a pirouette-kind of mechanism instead of via a retrocycloaddition starting from the [6,6] isomer.[14] Finally, an enhanced reactivity for the Diels−Alder and the 1,3-dipolar cycloaddition reactions was recently reported for the D_{5h} isomers of Sc$_3$N@C$_{80}$ and Lu$_3$N@C$_{80}$ as compared to the most common I_h isomers.[15] This D_{5h} isomer contains [6,6] pyracylene-type bonds, and, therefore,

similar to the reactivity of C$_{60}$, the reactions took place over these pyracylenic bonds. As to endohedral derivatives of C$_{78}$, Cai and co-workers[16] have recently synthesized the first *N*-tritylpyrrolidino derivatives of D_{3h}-Sc$_3$N@C$_{78}$. The adducts have been characterized by NMR experiments and X-ray crystallographic analyses which have shown that the reaction takes place over two different [6,6] type-B bonds (and not over the [6,6] pyracylenic bonds). Even more recently, Cao and co-workers[17] have reported thermal and photochemical addition reactions of adamantylidene to [6,6] and [5,6] bonds of La$_2$@C$_{78}$.

Campanera and collaborators[18] performed calculations at the BP86/TZP level for I_h-C$_{60}$, D_3-C$_{68}$, D_3-Sc$_3$N@C$_{68}$, D_{5h}-C$_{70}$, $D_{3h'}$-C$_{78}$, D_{3h}-Sc$_3$N@C$_{78}$, I_h-C$_{80}$, and several isomers of Sc$_3$N@C$_{80}$ metallofullerenes to find structural and/or orbital parameters that correctly indicate the most-reactive exohedral sites for the Diels−Alder reaction with 1,3-butadiene. On the basis of these studies, the most-reactive sites were those with a high Mayer bond order (MBO)[19] (higher MBOs are usually connected to shorter C−C bonds) and high pyramidalization angles. For Sc$_3$N@C$_{78}$, the authors[18] concluded that the most-reactive bond should be a [6,6] pyracylenic type-A bond (in particular bond **7**, see Figure 2) followed by two [6,6] type-B bonds (**6** and **4**); the other bonds (the rest of [6,6] and all [5,6] bonds) were discarded because of their lower MBOs and larger bond distances. As can be seen in Figure 2, the C$_{78}$ fullerene has seven nonequivalent [6,6]-type bonds that can be classified into three subtypes: pyracylenic or type A (bonds **1** and **7**); type B (bonds **3**, **4**, **5**, and **6**); and pyrenic or type C (bond **2**). Moreover, it has six nonequivalent [5,6]-type bonds that are corannulene or type D (bonds **a**, **b**, **c**, **d**, **e**, and **f**).

Detailed theoretical calculations are needed to determine the most-reactive sites of metallofullerenes because there is no clear evidence about the possible consequences of TNT encapsulation on the exohedral reactivity of metallofullerenes as two opposite effects counteract. First, the introduction of the metal cluster is likely to produce an increment of the pyramidalization of the carbon atoms. This leads to an increase of strain energy and, therefore, a higher reactivity of the cage. Second, the charge transfer from the metal cluster to the fullerene structure causes a reduction of the electron affinity, thus diminishing the reactivity of the endohedral compound. In addition, it is important to note that the effect of encapsulation may be different for the different bond types and is likely to depend on the type of metal compound present inside the cage. Although Campanera et al.[18] gave already some clues about the reactive sites of this compound, detailed theoretical calculations of the whole reaction channels are needed to fully determine the change in reactivity upon encapsulation for all different bond types and finally obtain a full and detailed description of the C$_{78}$ and Sc$_3$N@C$_{78}$ reactivity. Because experimental studies of the 1,3-dipolar cycloaddition over Sc$_3$N@C$_{80}$ showed that the thermodynamic and the kinetic products do not always cor-respond to the same adduct,[12] the kinetics of the reaction (i.e., the transition-state structure, which is experimentally unattain-

(9) Cardona, C. M.; Kitaygorodskiy, A.; Ortiz, A.; Herranz, M. A.; Echegoyen, L. *J. Org. Chem.* **2005**, *70*, 5092–5097.

(10) Cardona, C. M.; Kitaygorodskiy, A.; Echegoyen, L. *J. Am. Chem. Soc.* **2005**, *127*, 10448–10453.

(11) Chen, N.; Fan, L. Z.; Tan, K.; Wu, Y. Q.; Shu, C. Y.; Lu, X.; Wang, C. R. *J. Phys. Chem. C* **2007**, *111*, 11823–11828.

(12) Cai, T.; Slebodnick, C.; Xu, L.; Harich, K.; Glass, T. E.; Chancellor, C.; Fettinger, J. C.; Olmstead, M. M.; Balch, A. L.; Gibson, H. W.; Dorn, H. C. *J. Am. Chem. Soc.* **2006**, *128*, 6486–6492.

(13) (a) Echegoyen, L.; Chancellor, C. J.; Cardona, C. M.; Elliott, B.; Rivera, J.; Olmstead, M. M.; Balch, A. L. *Chem. Commun.* **2006**, 2653–2655. (b) Cardona, C. M.; Elliott, B.; Echegoyen, L. *J. Am. Chem. Soc.* **2006**, *128*, 6480–6485.

(14) Rodríguez-Fortea, A.; Campanera, J. M.; Cardona, C. M.; Echegoyen, L.; Poblet, J. M. *Angew. Chem., Int. Ed.* **2006**, *45*, 8176–8180.

(15) Cai, T.; Xu, L. S.; Anderson, M. R.; Ge, Z. X.; Zuo, T. M.; Wang, X. L.; Olmstead, M. M.; Balch, A. L.; Gibson, H. W.; Dorn, H. C. *J. Am. Chem. Soc.* **2006**, *128*, 8581–8589.

(16) Cai, T.; Xu, L.; Gibson, H. W.; Dorn, H. C.; Chancellor, C. J.; Olmstead, M. M.; Balch, A. L. *J. Am. Chem. Soc.* **2007**, *129*, 10795–10800.

(17) Cao, B.; Nikawa, H.; Nakahodo, T.; Tsuchiya, T.; Maeda, Y.; Akasaka, T.; Sawa, H.; Slanina, Z.; Mizorogi, N.; Nagase, S. *J. Am. Chem. Soc.* **2008**, *130*, 983–989.

(18) Campanera, J. M.; Bo, C.; Poblet, J. M. *J. Org. Chem.* **2006**, *71*, 46–54.

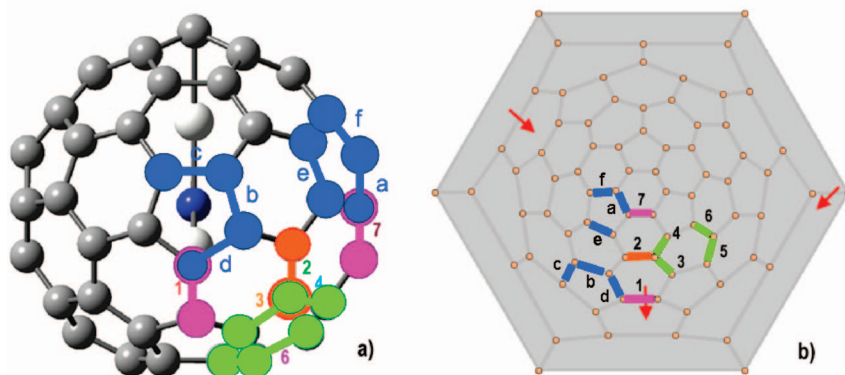(19) Mayer, I. *Chem. Phys. Lett.* **1983**, *97*, 270–274.

Figure 2. (a) The different nonequivalent bonds of $Sc_3N@C_{78}$ are represented, where numbers denote [6,6] bonds, and lower-case letters denote [5,6] bonds. Different colors are used to mark the different bond types (pink is for type A, green for type B, orange for type C, and blue for type D). (b) The Schlegel diagram of $Sc_3N@C_{78}$ is shown, which converts the 3D fullerene structure into a 2D representation. The positions of the scandium atoms facing the different bonds are symbolized with a red arrow.

able) is an important aspect to determine that has not been considered yet in previous works on metallofullerenes.

The aim of this study is therefore to investigate the change on the exohedral reactivity of free fullerene C_{78} when a metal cluster is encapsulated inside the cage. In particular, in this work, we analyze both the thermodynamics and the kinetics of the cycloaddition Diels−Alder reaction of 1,3-butadiene over all different bonds of C_{78} and $Sc_3N@C_{78}$. The choice of the C_{78} cage is in part motivated by the lack of free rotation of the Sc_3N unit inside the carbon cage (the BP86/TZP energy barrier for rotation of the Sc_3N moiety is as high as 25.8 kcal·mol^{-1}),[20] which facilitates the theoretical study and allows the evaluation of the change in reactivity for all nonequivalent bonds. This is in contrast to what is found for larger cages such as C_{80}, where the M_3N unit rotates freely, and consequently, the reduction of the reactivity of the [5,6] and [6,6] bonds due to the Sc_3N unit is similar because it is somehow averaged with the rotation of the Sc_3N unit.[21] To the best of our knowledge, a complete theoretical study of the reaction energies and barriers for all nonequivalent bonds of a given free and endohedral fullerene structure has never been done before. Hence, this project provides a detailed description of a concrete reaction, the results of which can serve as reference for future studies. In this way, a new step will be done to understand fullerene properties and reactivity, which could probably be useful for future medical and biological applications.

Computational Details

All density functional theory (DFT) calculations were performed with the Amsterdam density functional (ADF) program.[22,23] The molecular orbitals were expanded in an uncontracted set of Slater-type orbitals (STOs) of double-ζ (DZP) and triple-ζ (TZP) quality containing diffuse functions and one set of polarization functions. Core electrons (1s for second period and 1s2s2p for third period) were not treated explicitly during the geometry optimizations (frozen core approximation),[23] because it was shown to have a negligible

effect on the obtained geometries.[24] An auxiliary set of s, p, d, f, and g STOs was used to fit the molecular density and to represent the Coulomb and exchange potentials accurately for each self-consistent field cycle. Energies and gradients were calculated by using the local density approximation (Slater exchange and VWN correlation)[25] with nonlocal corrections for exchange[26] and correlation[27] included self-consistently (i.e., the BP86 functional). All energies reported here have been obtained with the TZP basis in single-point energy calculations at geometries that were obtained with the DZP basis (i.e., BP86/TZP//BP86/DZP). Although it is well-documented that standard DFT functionals such as BP86 underestimate energy barriers[28] (in the case of the parent Diels−Alder reaction, BP86/TZP predicts a barrier of 18.6 kcal·mol^{-1}, i.e., an underestimation of the experimental value by about 6 kcal·mol^{-1}), this underestimation should be similar for all Diels−Alder transition states (TSs) we encounter here. In addition, we have verified that the trends, that is, reaction energies and barriers, reported here do not change when using different DFT functionals.

The actual geometry optimizations and TS searches were performed with the QUILD[29] (quantum-regions interconnected by local descriptions) program, which functions as a wrapper around the ADF program. The QUILD program constructs all input files for ADF, runs ADF, and collects all data; ADF is used only for the generation of the energy and gradients. Furthermore, the QUILD program uses improved geometry-optimization techniques, such as adapted delocalized coordinates[29] and specially constructed model Hessians with the appropriate number of eigenvalues.[29] The latter is of particular use for TS searches. All TSs have been characterized by computing the analytical[30] vibrational frequencies, to have one (and only one) imaginary frequency corresponding to the approach of the two reacting carbons.

Results and Discussion

The Diels−Alder reaction between 1,3-butadiene and the fullerenes C_{78} and $Sc_3N@C_{78}$ has been studied in detail for all nonequivalent bonds of the fullerene. We will refer to each different bond according to the nomenclature used in Figure 2,

(20) Campanera, J. M.; Bo, C.; Olmstead, M. M.; Balch, A. L.; Poblet, J. M. *J. Phys. Chem. A* **2002**, *106*, 12356−12364.
(21) (a) Duchamp, J. C.; Demortier, A.; Fletcher, K. R.; Dorn, D.; Iezzi, E. B.; Glass, T.; Dorn, H. C. *Chem. Phys. Lett.* **2003**, *375*, 655−659. (b) Slanina, Z.; Nagase, S. *ChemPhysChem* **2005**, *6*, 2060−2063.
(22) Baerends, E. J. et al. ADF 2006.01; SCM: Amsterdam, 2006.
(23) te Velde, G.; Bickelhaupt, F. M.; Baerends, E. J.; Fonseca Guerra, C.; van Gisbergen, S. J. A.; Snijders, J. G.; Ziegler, T. *J. Comput. Chem.* **2001**, *22*, 931−967.

(24) Swart, M. S.; Snijders, J. G. *Theor. Chem. Acc.* **2003**, *110*, 34−41.
(25) Vosko, S. H.; Wilk, L.; Nusair, M. *Can. J. Phys.* **1980**, *58*, 1200−1211.
(26) Becke, A. D. *Phys. Rev. A* **1988**, *38*, 3098−3100.
(27) Perdew, J. P. *Phys. Rev. B* **1986**, *33*, 8800−8802.
(28) Swart, M.; Solà, M.; Bickelhaupt, F. M. *J. Comput. Chem.* **2007**, *28*, 1551−1560.
(29) (a) Swart, M.; Bickelhaupt, F. M. *Int. J. Quantum Chem.* **2006**, *106*, 2536−2544. (b) Swart, M.; Bickelhaupt, F. M. *J. Comput. Chem.* **2008**, *29*, 724−734.
(30) Wolff, S. K. *Int. J. Quantum Chem.* **2005**, *104*, 645−659.

Table 1. Reaction Energies ΔE_R and Bond Lengths in the Cycloaddition Products of the C—C Bonds over Which the Reaction Took Place (R_{full}) and of the New C—C Bonds Formed (R_{CC})[a]

product	bond type	ΔE_R (kcal·mol⁻¹)	R_{full} (Å)	R_{CC} (Å)		ΔE_R (kcal·mol⁻¹)	R_{full} (Å)	R_{CC} (Å)	
			C₇₈				Sc₃N@C₇₈		
1	A [6,6]	**−16.0**	1.552	1.582	1.582	+4.0	1.605	1.572	1.572
2	C [6,6]	+12.5	1.696	1.581	1.581	+6.1	1.681	1.578	1.578
3	B [6,6]	+1.8	1.625	1.577	1.581	+9.2	1.675	1.570	1.573
4	B [6,6]	−9.2	1.624	1.573	1.577	**−9.7**	1.639	1.564	1.576
5	B [6,6]	+0.9	1.604	1.574	1.590	+5.9	1.613	1.575	1.581
6	B [6,6]	+4.0	1.609	1.571	1.586	**−12.7**	1.584	1.570	1.572
7	A [6,6]	**−18.8**	1.580	1.574	1.574	−7.6	1.585	1.574	1.574
a	D [5,6]	−8.8	1.622	1.566	1.566	−6.0	1.628	1.563	1.563
b	D [5,6]	**−23.9**	1.612	1.566	1.570	−4.3	1.637	1.561	1.568
c	D [5,6]	−13.3	1.608	1.568	1.568	**−10.4**	1.621	1.563	1.563
d	D [5,6]	−5.2	1.604	1.561	1.570	−7.6	1.656	1.559	1.563
e	D [5,6]	−13.8	1.625	1.566	1.569	−4.9	1.637	1.563	1.564
f	D [5,6]	−5.9	1.594	1.567	1.570	−6.5	1.611	1.563	1.564

[a] Boldface font: bonds that are most reactive under thermodynamic control.
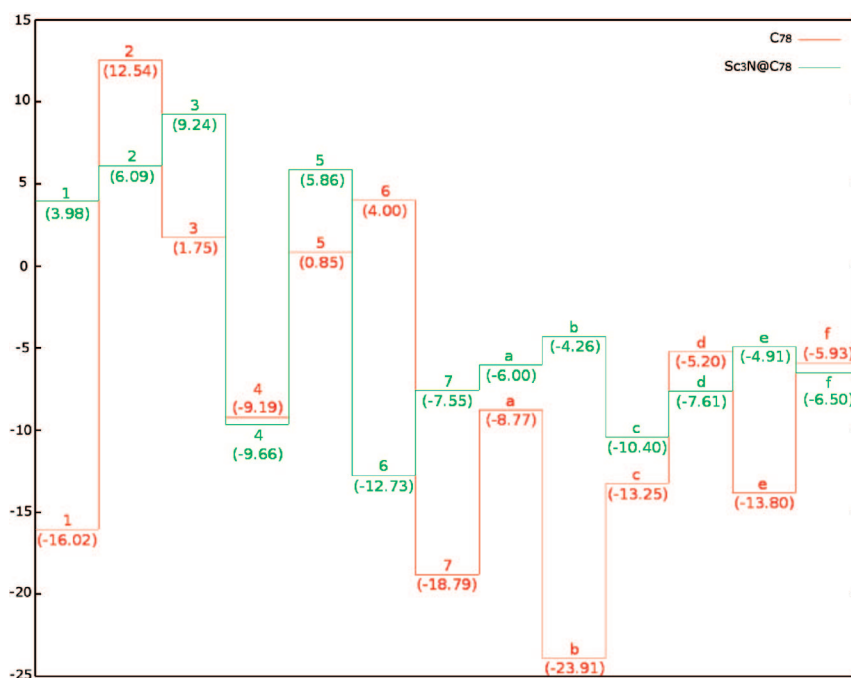
Figure 3. Comparison between the reaction energies (kcal·mol⁻¹) in the free fullerene C₇₈ (in red) and endohedral fullerene Sc₃N@C₇₈ (in green), where numbers denote [6,6] bonds, and lowercase letters are used for [5,6] bonds.

where for example, **1** is used to denote the [6,6] pyracylenic or type-A bond situated in the position as indicated in Figure 2, and **a** refers to the [5,6] corannulene or type-D bond, the situation of which is also marked in the same figure.

Reaction Energies for Diels—Alder Reaction on Nonequivalent Bonds. The reaction energies at the BP86/TZP//BP86/DZP level listed in Table 1 show some clear differences for the different types of bonds in free fullerene. The reaction energy for the [5,6] bonds is in all cases exothermic but is found in a wide range, from −5 to −24 kcal·mol⁻¹. The most-exothermic reaction energy is obtained when the attack is produced over bond **b** (−23.9 kcal·mol⁻¹, see Table 1), whereas the least-exothermic [5,6] bonds are **d** and **f** (ca. −5 kcal·mol⁻¹). For C₆₀, it was shown that the most-reactive bonds are the [6,6] pyracylenic or type-A bonds, which are also present in the C₇₈ fullerenes studied here. Therefore, it might have been expected that they may lead to the most-stable products. Indeed, among the different [6,6] bonds in free fullerene, the pyracylenic type-A bonds are the most reactive, with values for the reaction energy

of −16.0 (**1**) and −18.8 (**7**) kcal·mol⁻¹. The type-B bonds are, with the exception of bond **4** (that has a reaction energy of −9.2 kcal·mol⁻¹), all slightly endothermic (1−4 kcal·mol⁻¹). Least reactive of all is however bond **2**, of type C (see Figure 1), which is endothermic by 12.5 kcal·mol⁻¹.

For the endohedral compound, the reactivity trend changes completely (see Figure 3). In general, the difference in reaction energy among the bonds is reduced, and therefore, the reaction is less regioselective. The three most-exothermic products of the free fullerene are significantly destabilized (by 12−20 kcal·mol⁻¹), whereas bond **6** of type B, which was endothermic for the free fullerene, is stabilized by ca. 17 kcal·mol⁻¹ to become the most-exothermic product for Sc₃N@C₇₈ (−12.7 kcal·mol⁻¹, see Table 1). Together with bond **4**, which provided already an exothermic product in the free fullerene (of almost equal stability, i.e., −9.2 kcal·mol⁻¹ in free fullerene versus −9.7 kcal·mol⁻¹ in the endohedral derivative), and bond **7** (−7.6 kcal·mol⁻¹), these are the only [6,6] bonds giving exothermic products. The other four [6,6] bonds (**1**, **2**, **3**, and

Table 2. Reaction Barriers and Distances for the C−C Bonds Being Formed at the TS[a]

product	bond-type	C78			Sc3N@C78		
		TS	$\Delta E^{\ddagger}$ (kcal·mol⁻¹)	R_{CC} (Å)	TS	$\Delta E^{\ddagger}$ (kcal·mol⁻¹)	R_{CC} (Å)
1	A [6,6]	syn	**12.2**	2.253	2.259	asyn	23.8	1.762	2.457
2	C [6,6]	asyn	30.2	1.717	2.422	asyn	27.1	1.699	2.525
3	B [6,6]	asyn	21.7	1.653	2.499	asyn	28.9	1.715	2.465
4	B [6,6]	asyn	14.8	1.945	3.086	asyn	**20.0**	1.995	2.507
5	B [6,6]	asyn	14.4	1.927	3.157	asyn	27.6	1.758	2.496
6	B [6,6]	asyn	17.2	1.847	3.193	asyn	**18.5**	2.077	2.415
7	A [6,6]	syn	**13.5**	2.271	2.278	syn	**20.1**	2.164	2.215
a	D [5,6]	asyn	17.2	1.866	3.029	asyn	21.5	1.804	2.761
b	D [5,6]	asyn	**12.5**	2.130	2.616	asyn	**20.7**	1.673	2.664
c	D [5,6]	asyn	16.7	1.907	3.731	asyn	**20.1**	1.926	2.622
d	D [5,6]	asyn	22.1	1.695	2.713	asyn	**19.7**	1.851	2.649
e	D [5,6]	asyn	15.3	1.960	2.943	asyn	22.3	1.750	2.758
f	D [5,6]	asyn	18.0	1.874	3.372	asyn	21.5	1.784	2.927

[a] Boldface font: bonds that are most reactive under kinetic control.

5) give significantly endothermic products (4−9 kcal·mol⁻¹). It is worth mentioning here that the reaction energies for the same cycloaddition reaction on bonds **4**, **6**, and **7** were already reported by Campanera and co-workers,[18] and the same reactivity order (**6** > **4** > **7**) was obtained.

Similar to free fullerene, all [5,6] bonds in Sc3N@C78 provide exothermic products but with a smaller range of stability (−4 to −10 kcal·mol⁻¹) and in a different order. The most exothermic [5,6] products are now resulting from addition to bonds **c** and **d** (−10.4 and −7.6 kcal·mol⁻¹, respectively). Interestingly, the reaction over bond **c** leads to the second most favorable reaction energy (only bond **6** is more stable, see Table 1), which is in contrast with what Campanera and co-workers predicted.[18,31] Two [5,6] bonds enhance their stability slightly (bonds **d** and **f**), whereas the others become more endothermic upon TNT encapsulation.

A comparison of the reaction energies for both free and endohedral fullerene reveals that C78 products have, in general, more-favorable reaction energies; therefore, C78 reactivity is clearly reduced when the TNT unit is introduced (see Figure 3). Although products **2**, **d**, and **f** have slightly more-favorable reaction energies after the TNT encapsulation, the only product for which the reaction energy is clearly enhanced is **6** (with a reaction energy value of 4.0 kcal·mol⁻¹ in C78 and −12.7 kcal·mol⁻¹ in Sc3N@C78), whereas a significant decrease in exothermicity is produced in the other products. The most important destabilization is found for products **1** and **b**, the reaction energy value of which is reduced by 20 kcal·mol⁻¹, and products **3**, **7**, and **e** with a reduction of 8−11 kcal·mol⁻¹. In general, the bonds that are more deactivated are those located closer to one of the Sc atoms of the Sc3N unit (with the exception of bond **d**, which is close to a Sc, but its reaction energy is not affected).

Energy Barriers. We have also determined the TS structures for the cycloaddition reaction, for each of the nonequivalent bonds, and for both free and endohedral fullerenes. In all cases, the TS search has started from a symmetric structure in which the two C−C bonds to be formed have the same bond length, leading, in most cases, to an asynchronic TS (even in the symmetric addition sites, where the synchronic TS is actually a second-order saddle point).[32]

(31) Akasaka, T.; Nagase, S. *Endofullerenes: A new Family of Carbon Clusters*; Kluwer Academic Publishers: Dordrecht, 2002.
(32) Bachrach, S. M.; White, P. B. *J. Mol. Struct.: THEOCHEM* **2007**, *819*, 72–78.

In the free fullerene case, the three most-exothermic products (**1**, **7**, and **b**) also have the lowest barriers, but in different order (see Table 2). The lowest barrier (12.2 kcal·mol⁻¹) is observed for the third most-exothermic product (**1**), followed by the most-exothermic product (**b**, barrier 12.5 kcal·mol⁻¹), and product **7** with a barrier of 13.5 kcal·mol⁻¹. The other TSs are found at slightly higher energies (14.4−18.0 kcal·mol⁻¹) or considerably higher energies (21.7−30.2 kcal·mol⁻¹). The highest barrier is observed for bond **2**, which also provided the most-endothermic product for the free fullerene.

In the Diels−Alder reaction between Sc3N@C78 and 1,3-butadiene, the favored product under thermodynamic control (**6**) is also the favored product under kinetic control with a barrier of 18.5 kcal·mol⁻¹. Note that this corresponds to an increase of 6 kcal·mol⁻¹ with respect to the reaction with the lowest barrier in free fullerene, and this is now almost the same energy as that of the parent Diels−Alder reaction between butadiene and ethylene, for which BP86/TZP predicts a barrier of 18.6 kcal·mol⁻¹ (18.9 kcal·mol⁻¹ at the BP86/TZ2P). This loss of reactivity is a general trend observed for all bonds; in fact, only bonds **2** and **d** have lower energy barriers upon TNT encapsulation (see Figure 4), whereas the others show an increase by up to 13 kcal·mol⁻¹.

The low barrier of bond **6** is followed by a group of five other bonds (**4**, **7**, **b**, **c**, and **d**) that are found within a range of 1 kcal·mol⁻¹ (19.7−20.7 kcal·mol⁻¹) from each other, a second group with the other [5,6] bonds (**a**, **e**, and **f**) at ca. 22 kcal·mol⁻¹, and finally the other [6,6] bonds at 24−29 kcal·mol⁻¹ (see also Figure 4). It is interesting to note that the first N-tritylpyrrolidino derivatives of Sc3N@C78 synthesized by Cai et al.[16] were the result of the addition of the azomethine ylides to bonds **4** and **6** (bonds **b**−**d** and **c**−**f**, respectively, in the work by Cai et al.[16]), which are the two most-reactive [6,6] bonds according to the present calculations. Our results, however, also predict the possible formation of the [5,6] adduct **c** for the Diels−Alder cycloaddition of Sc3N@C78 with 1,3-butadiene (**7** and **d** could also be formed, but they are thermodynamically less favored).

More conclusions may be drawn by looking at the C−C bond distances in the TSs for the bonds to be formed (see Table 2). There does not seem to be a direct relationship between the reaction barrier and the (a)synchronicity of the TS structure. For instance, although the lowest energy barrier in free fullerene corresponds to a synchronous structure with the two forming bonds of similar magnitude, there is only one other synchronous TS observed for free and endohedral fullerene (**1** and **7**). All
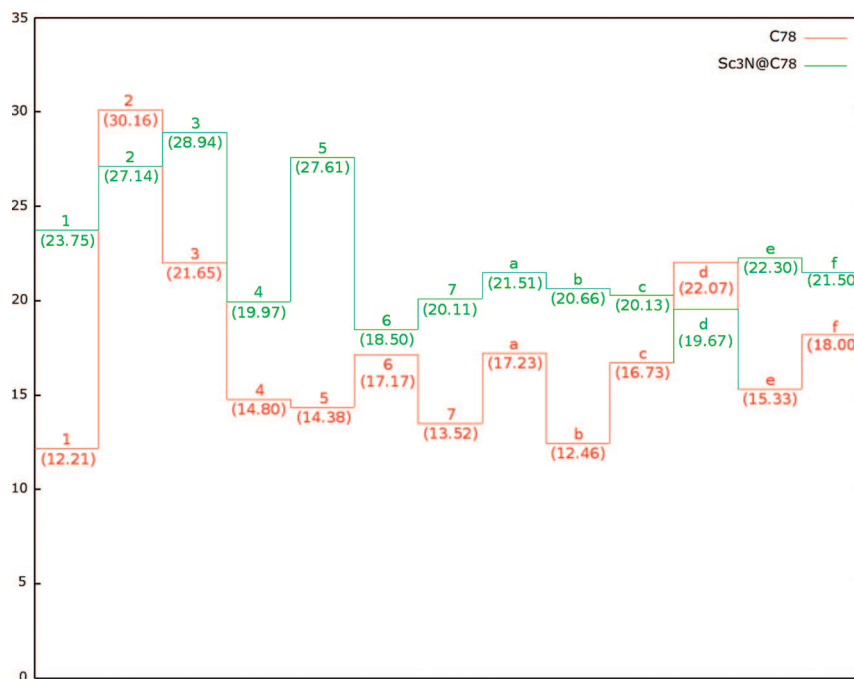
Figure 4. Comparison between the activation energies (kcal·mol^{-1}) in the free fullerene C$_{78}$ (in red) and endohedral fullerene Sc$_3$N@C$_{78}$ case (in green), where numbers denote [6,6] bonds, and lower case letters are used for [5,6] bonds.
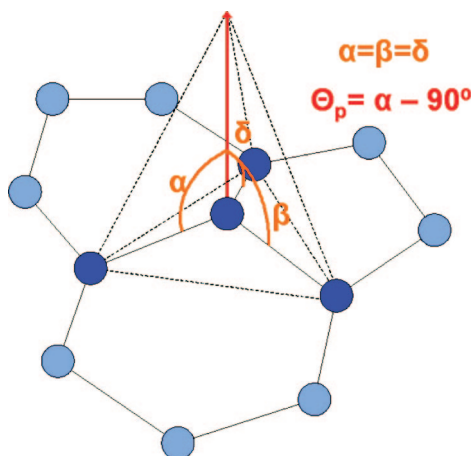

Figure 5. Representation of the pyramidalization angle. A vector that equalizes the angles α, β, and δ is defined in order to compute the final pyramidalization angle value ($\theta_p = \alpha - 90°$).

Table 3. Bond Distances and Pyramidalization Angles for the Bond Types in Free and Endohedral Fullerenes[a]

product	bond-type	C$_{78}$		Sc$_3$N@C$_{78}$	
		R_{CC} (Å)	θ_p (°)[b]	R_{CC} (Å)	θ_p (°)[b]
1	A [6,6]	**1.369**	10.46	1.440	**13.80**
2	C [6,6]	1.465	8.58	1.466	8.33
3	B [6,6]	1.432	9.62	1.450	9.26
4	B [6,6]	1.415	9.60	**1.426**	9.44
5	B [6,6]	1.418	9.53	1.432	8.97
6	B [6,6]	1.420	9.44	**1.400**	9.99
7	A [6,6]	**1.388**	**11.64**	**1.400**	**11.21**
a	D [5,6]	1.438	**11.64**	1.437	**11.21**
b	D [5,6]	**1.410**	10.49	1.446	9.73
c	D [5,6]	1.465	10.32	**1.423**	9.27
d	D [5,6]	1.446	10.56	1.452	**12.00**
e	D [5,6]	1.438	10.38	1.449	10.92
f	D [5,6]	1.442	**11.13**	1.432	10.88

[a] Boldface font: the bonds that are predicted to be most reactive. [b] Pyramidalization angles averaged over both atoms that constitute the bond under consideration.

the other TSs are modestly ($\Delta R_{CC} = 0.4-0.7$ Å) to significantly ($\Delta R_{CC} = 1.0-1.6$ Å) asynchronous.[32]

Reactivity Predictions Based on Bond Distances, Pyramidalization Angles, and Shapes of the Lowest-Lying Unoccupied Molecular Orbitals. As pointed out in previous works,[33] the Diels–Alder reaction should be favored over bonds that have short bond distances and high pyramidalization angles θ_p. This pyramidalization angle (see Figure 5), introduced by Haddon,[34] is a measure of the local curvature in polycyclic aromatic hydrocarbons, which differentiates in a simple manner between, for example, sp^2 ($\theta_p = 0°$) and sp^3 ($\theta_p = 19.47°$) centers. Shorter bonds with higher pyramidalization angles are favored for two reasons: first, because they exhibit more double-

(33) Solà, M.; Mestres, J.; Duran, M. *J. Phys. Chem. A* **1995**, *99*, 10752–10758.
(34) (a) Haddon, R. C. *J. Phys. Chem. A* **2001**, *105*, 4164–4165. (b) Haddon, R. C.; Chow, S. Y. *J. Am. Chem. Soc.* **1998**, *120*, 10494–10496.
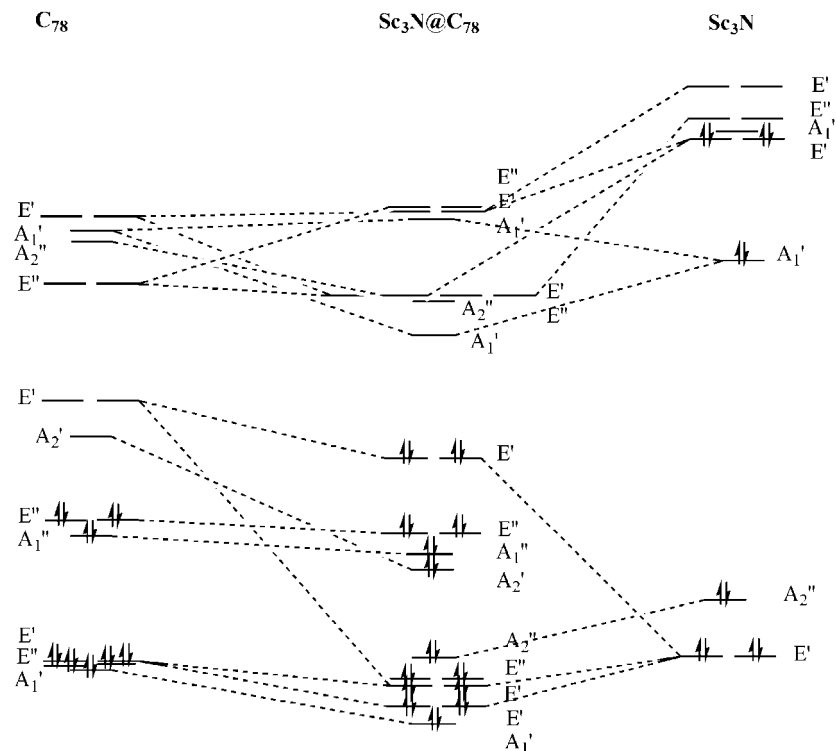
bond character that facilitates the interaction with the diene, and second, because the higher the pyramidalization, the closer to the final sp^3 geometry, and hence, the system has to be deformed less during its transit from reactants to TS or products. In Table 3, we report the pyramidalization angles as well as bond distances for all considered bonds, both for free C$_{78}$ and encapsulated Sc$_3$N@C$_{78}$, so that we can compare these predictors with the observed kinetic and thermodynamic reactivity.

In the free fullerene case, type-A bonds **1** and **7** exhibit the shortest bond distances (1.37–1.39 Å), followed by [5,6]-bond **b** (1.41 Å). The reaction energies as well as the activation barriers of the free fullerene agree well with the predicted trends based on bond distances, which predicted indeed **1**, **7**, and **b** to be most reactive (although in a different order). Likewise, the endothermicity of bond **2** of +13 kcal·mol^{-1} concurs well with its large bond distance of 1.47 Å. However, bond **c** has a similarly large distance (1.47 Å) but provides a considerably exothermic product (−13 kcal·mol^{-1}). In fact, all [5,6]-bond

Figure 6. Molecular orbital level diagram of the free fullerene, Sc_3N, and $Sc_3N@C_{78}$ orbitals.

distances are relatively large (1.44−1.47 Å, apart from bond **b**), yet each one of them provides a modest-to-significant exothermic product. For the endohedral compound, the three most exothermic products (**4**, **6**, and **c**) do indeed have small bond distances, with the most exothermic product (**6**) having the smallest distance (see Tables 1−3). But bond **7** is of equal length (1.40 Å), and yet, it is less exothermic by 5 kcal·mol^{-1}. Likewise, the bond with the largest distance (**2**, 1.47 Å) does not provide the most-endothermic product. Therefore, there is no overall correlation between the bond-distance predictions and the actual reaction energies found in both cases.

Using the pyramidalization angle as predictor for reactivity gives even worse results. Although some predictions concur with the actual reaction energy in C_{78} (like bond **2**, which has the smallest pyramidalization angle and indeed the largest endo-thermic reaction energy), there is no overall agreement. For instance, bond **f**, with one of the largest angles (11.1°), shows only a modest exothermic reaction of −6 kcal·mol^{-1}. In the endohedral fullerene, the bond with the largest angle (bond **1**, 13.8°) is endothermic (4.0 kcal·mol^{-1}), whereas the most exothermic product results from a bond which is only modestly pyramidalized.

Apart from the structural predictors (bond distance and pyramidalization angle), we also explored the molecular orbitals of the reactant fullerenes as possible descriptor for the observed reactivity. In the case of free fullerene and its endohedral derivative, the main interactions occur between the highest occupied molecular orbital (HOMO) of butadiene (at −5.77 eV) and the lowest unoccupied molecular orbitals (LUMOs) of the fullerene (found between −5.13 and −4.86 eV for C_{78} and between −4.20 and −3.87 eV for $Sc_3N@C_{78}$). Note that because of the formal charge transfer upon metal-cluster encapsulation, the three lowest LUMOs of the free fullerene are occupied and only higher-lying unoccupied orbitals are available for interact-ing with the HOMO of the diene (see Figure 6). As a result,

the HOMO(diene)−LUMO(dienophile) gap increases from 0.64 eV for free fullerene to 1.57 eV for the endohedral derivative. This larger gap should lead to a reduced interaction and, hence, a reduced reactivity, which is indeed what we observe.

If we now study in more detail the low-lying unoccupied orbitals of either the free fullerene cage or the endohedral derivative, some additional predictions about their exohedral reactivity might be made. Of course, the larger the contributions of the C atoms for a certain C−C bond in the LUMOs, the more reactive the bond will be. But the lobes of the LUMOs within any one of these bonds should be of opposite sign in order to facilitate the [4 + 2]-cycloaddition reaction. In the C_{78} case, bonds **1**, **7**, and **b** have suitable orbitals to interact with the HOMO of the diene (see Figure 7); they are indeed the three most-exothermic bonds we observed (see Table 1). Bonds **4** and **e** are also predicted to be reactive, which came next in terms of exothermicity.

In $Sc_3N@C_{78}$, bonds **1**, **2**, **3**, **4**, **6**, **7**, **c**, and **e** present favorable orbitals to react with (see Figure 8), whereas the most-exothermic reaction energies were obtained for products **6**, **c**, **4**, **7**, and **d** (see Table 1). Thus, the LUMO criterion fails to predict the nonreactivity in bonds **1**, **2**, and **3** that correspond to endothermic reactions. Therefore, the predictions of reactivity from the LUMOs are qualitatively correct but much too imprecise in the sense that one finds many bonds with suitable orbitals for the interaction with the HOMO of 1,3-butadiene.

Finally, let us conclude that a combination of the three criteria proves to be quite successful to predict the chemical reactivity of the different bonds. Thus, in C_{78}, only bonds **1**, **7**, and **b** have small C−C bond lengths, relatively high pyramidalization angles, and suitable orbitals to interact with the HOMO of the diene. Similarly, for $Sc_3N@C_{78}$, only bonds **4**, **6**, **7**, **c**, and **d** obey the three criteria, and they correspond indeed to the most-exothermic reactions (the only exception could be **1**, but its C−C bond length is relatively large for a [6,6] bond, and only the
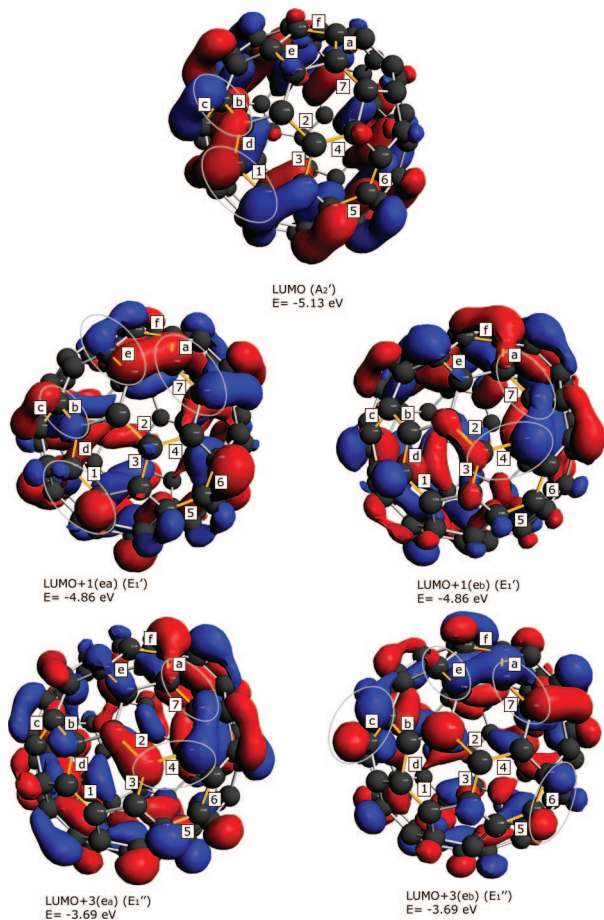
Figure 7. Representation of the C$_{78}$ LUMO, LUMO+1, and LUMO+3 molecular orbitals (isosurface value 0.02 au) where all nonequivalent [6,6] and [5,6] bonds have been marked. Those bonds with favorable orbitals to interact with the HOMO of the diene are marked with ellipses.

LUMO+4(e$_a$) at −3.87 eV has the correct shape to interact with the HOMO of the diene in this bond). It is interesting to note that bond **6** suffers a significant reduction of the C−C bond length and a slight increase in the pyramidalization angle (see Table 3) when going from free to encapsulated fullerene, although at the same time, this bond remains far from the influence of the TNT unit in Sc$_3$N@C$_{78}$ (see Figure 2).

Final Remarks and Conclusions

Theoretical calculations have revealed that not only is Sc$_3$N@C$_{78}$ less reactive, but it also has a different reactivity than its free derivative C$_{78}$. In this sense, the decrease of the exohedral reactivity represents an improvement for future medical applications with respect to the free cage, because it would make the process safer, and secondary reactions with biomolecules would probably be reduced. However, Sc$_3$N@C$_{78}$ still presents energy barriers of the same magnitude as that of the parent Diels−Alder reaction (ca. 19 kcal·mol^{-1} at BP86/TZP). Other TNT units with different metals (e.g., Y$_3$N or Sc$_2$YN) might lead to even less-reactive compounds with higher activation energies, which could therefore be more appropriate for medical purposes.

The introduction of the metal cluster Sc$_3$N inside the fullerene cage leads to several changes of the physical properties of the compound. The main reactivity differences are due to the changes produced in the low-lying unoccupied orbitals, which should be suitable to interact with the diene. The presence of
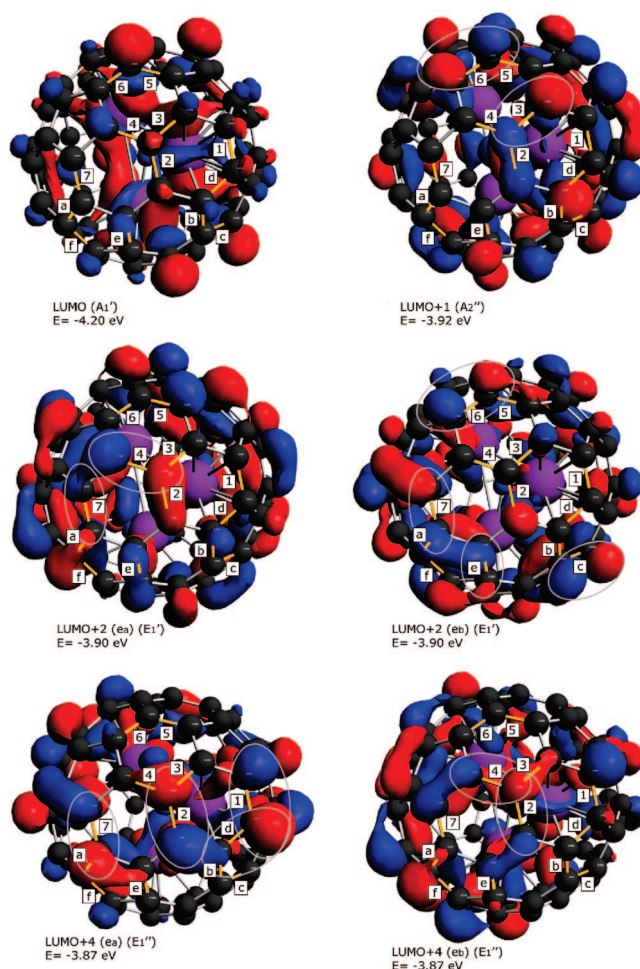

Figure 8. Representation of the Sc$_3$N@C$_{78}$ LUMO, LUMO+1, LUMO+2, and LUMO+4 molecular orbitals (isosurface value 0.02 au) where all nonequivalent [6,6] and [5,6] bonds have been marked. Those bonds with favorable orbitals to interact with the HOMO of the diene are marked with ellipses.

the metal cluster leads to a formal charge transfer from the cluster to the fullerene. As a result, the three LUMOs of the free fullerene are occupied in the endohedral compound, and only higher-lying unoccupied orbitals are available for interacting with the HOMO of the diene. This results in a larger HOMO(diene)−LUMO(dienophile) gap, with a corresponding decrease of reactivity.

For the free fullerene, the product under thermodynamic control is obtained for the cycloaddition to the [5,6] bond **b**, whereas under kinetic control, it corresponds to the pyracylenic [6,6] bond **1**. In the case of the endohedral compound, both the kinetic and thermodynamic products correspond to addition to the type-B [6,6] bond **6**. However, both the exothermicity and reaction barriers indicate a significant reduction in reactivity for the endohedral compounds compared to that of the free fullerene. In addition, the reaction energy differences among the different attacks are reduced in Sc$_3$N@C$_{78}$, thus indicating a reduction of the regioselectivity of the reaction due to Sc$_3$N encapsulation.

The reactivity patterns obtained in the study of the kinetics and thermodynamics of the different attacks do not correlate well with the predictions based on bond lengths, pyramidalization angles, and LUMOs shapes and energies. Some agreement is observed, for instance, the fact that the three shortest bonds

in the free fullerene correspond to the three most-stable products with the lowest barrier. However, of these three bonds, it is the one with the largest distance that is the most exothermic. Similar inconsistencies are observed for the other bonds and the endohedral compound. Moreover, in several instances, we observe different predictions from the bond distance versus the pyramidalization angle. In general, orbital studies give a good, although somewhat imprecise, approximation to the fullerene reactivity, because those bonds with LUMOs that are unsuitable for the interaction with the HOMO of the diene will surely produce less-stable products with higher barrier energies. However, the presence of suitable orbitals is not enough to ensure that the final product will be stable and will present low barrier energies, because other factors such as bond distances and pyramidalization do also contribute. Indeed, the combination of short bond lengths, high pyramidalization angles, and appropriate shape of some of the LUMOs provide the best criterion for chemical-reactivity predictions. Still, an exploration of the complete energy profile remains mandatory for the understanding of the modulation of the chemical reactivity of these fascinating compounds.

It is important to mention that although [5,6] bonds have been considered to be much less reactive in those structures possessing [6,6]-pyracylene-type bonds, the present study has also shown that the reaction energies as well as the activation barriers for certain [5,6] bonds are favorable and might play an important role in the fullerene exohedral reactivity. Finally, we note that the present conclusions are relevant for the C_{78} fullerene, where the influence of the metal unit inside the cage on the reactivity can be studied in great detail. But they cannot be extrapolated in a straightforward manner to larger cages, where the metal unit may rotate freely, nor to different types of reaction.

Note Added in Proof. During preparation of the galley proof of the present paper, the following work discussing the selective formation of a symmetric $Sc_3N@C_{78}$ bisadduct via a Bingel-Hirsch reaction has appeared: Cai, T.; Xu, L.; Shu, C.; Champion, H. A.; Reid, J. E.; Anklin, C.; Anderson, M. R.; Gibson, H. W.; Dorn, H. C. *J. Am. Chem. Soc.* **2008**, *130*, 2136–2137.

Supporting Information Available: Table S1 with the BP86/DZP optimized Cartesian *xyz* coordinates (in Å) of all analyzed species and full details of ref 22. This material is available free of charge via the Internet at http://pubs.acs.org.

JA711167V